# Deliverable 3.1
## An optimized comprehensive diffusion MRI protocol

## Short Background

Existing microstructure imaging techniques require high imaging gradient strength and long imaging time, which limit their application to fixed tissue samples. To realize the potential of microstructure imaging in routine clinical studies, it is critical to identify the optimized acquisition protocol that is clinically acceptable and provides robust microstructure estimates. Existing microstructure imaging techniques assume a single orientation of axons, which limit their application to only the most coherently oriented white matter structures, such as the corpus callosum. For most other white matter areas, axons spread or bend, resulting in significant dispersion in axonal orientation distribution. The existing techniques will lead to an overestimation of axon diameters in such areas. Simulation experiments are a crucial step in the assessment of such new protocols before being tested on clinical scanners. Therefore, the aims of this part of the WP are to optimize acquisition protocols for microstructure estimation and also to use detailed simulation and phantom experiments to evaluate the existing and developing acquisition protocols for microstructure imaging.

White matter fibre-bundle tractography allows for non-invasive probing of white matter anatomical pathways connecting different grey matter functional regions. Tractography methods rely on underlying models of local water diffusion processes inside white matter. Traditionally, these processes have been described by the Gaussian tensor model. While tensorial representation proves adequate in characterizing diffusion for single fibre populations made of parallel fibres, it fails to capture the complexity of processes in more intricate fibre constellations (crossing fibres, kissing or bending fibres, etc.). Over the last decade, a plethora of non-Gaussian models obtained through HARDI signal analysis have been proposed. These models introduced significant improvements in describing diffusion processes in complicated environments, and enhanced the power of tractography methods. Nonetheless, intrinsic Bessel blurring still limits the angular resolution (i.e., "angular separation"), and typically used spherical harmonics bases put constraints on the minimum size of data needed to represent local diffusion processes. While orientational non-Gaussian distribution proves rather useful for tractography, interesting features may be missed by limiting the data investigation to a single shell. Multiple-shell analysis offers more elaborate depiction of the underlying diffusion process, and offers the possibility to deduce the information on the whole 3D diffusion propagator. Therefore, this part of the WP aims to develop sparse and sharp models for single-shell HARDI analysis, and three-dimensional models for multiple-shell HARDI analysis.

## Goals

The goals of this part of the project are:

- **Data analysis and acquisition optimization.** This will be achieved by: (A) Developing a framework for running diffusion simulations with virtual tissue environments constructed from microscope images of real tissue. (B) Comparison of simulation results with 9.4T measurements from the same sample to provide insight into which tissue parameters affect the signal. (C) Analysis of the data set collected in WP1 to assess how different acquisition

protocols may influence extracted microstructure parameters. (D) Developing methods to model the diffusion process using single-shell and multiple-shell high-angular resolution diffusion imaging. (E) Implementing optimal pulse sequences for imaging at ultra-high fields.

- **Analysis Routines Optimization.** This will be achieved by: (A) Optimizing the microstructure fitting routines, by incorporating further important parameters to the model to account for dispersion in axonal-orientation distribution. (B) Development of tissue mimetic materials for use in phantoms for validating tissue microstructure and tractography analyses and adapting the experimental conditions.

# Main Results

### (A) Data Analysis and Acquisition Optimization

Developing a diffusion signal simulation frameworks

To help identify the minimal acquisition scheme required for robust estimation of microstructure features, the group of DA developed a framework that simulates diffusion process in virtual tissue environments constructed from images of real tissue collected using high-resolution confocal laser scanning microscopy. The framework enables simulation of diffusion in an environment that mimics real tissue with high fidelity not previously possible. We were able to compare the simulation results to measurements acquired at 9.4T from the same tissue sample used to construct the virtual environment. The findings from this comparison give insight into the microstructure features that affects signal, which in turn leads to a better understanding of the most relevant signals to acquire that give the most sensitivity to such microstructure features. The group of DA has Extended the simulation from entirely synthetic tissue environments built from simple geometric primitives such as cylinders and spheres to more realistic environments derived from confocal image stacks of real tissue samples. Findings demonstrate that the additional detail provides synthetic data that matches measured MR data more closely than simple geometric models.

In addition, the group of DA runs simulation experiments on PGSE-based acquisition protocols with various maximum gradient strengths to determine the influence of gradient strength on the estimates of axon density and diameter. The findings, confirmed with measurements from fixed monkey brain, suggest the axon diameter estimates are sensitive to the available maximum gradient strength but becomes consistent when the maximum gradient strength becomes sufficiently high (above 140 mT/m).

The group of DB has worked on a novel simulation tool dedicated to diffusion-weighted (DW) MR experiments (Figure 1). The DB group combines a Monte Carlo Brownian dynamics simulator capable of simulating diffusion of spins in arbitrarily complex geometries with a DW signal integrator emulating various MR pulse sequences. The flexibility and ability of Monte-Carlo modeling enables the investigation of detailed dynamics and mechanisms of molecular diffusion in complex systems which cannot be handled through analytical models. Hence, we have developed software to reproduce various tissue configurations using dynamic meshes. Complicated geometries mimicking neural tissue components, such as neurons, astrocytes, axons, etc. can be emulated, as well as tissue features (e.g. cell size, density, membrane permeability) and basic diffusion mechanisms in different compartments (presence of attractors, local viscosity, membrane interactions, etc.). This framework allows bridging of the gap between elementary processes occurring at a micrometer scale and the resulting DW signal

measured at millimeter scale, providing a better understanding of the features observed in DW MRI (variation of apparent diffusion coefficient (ADC) with cell size, diffusion anisotropy) and to optimize acquisition schemes for different applications (e.g. fibre-tracking algorithms).

Using the tool presented in Figure 1, Simulations were performed using a random walk Monte Carlo simulator to simulate 3D water molecular diffusion in a bundle of parallel impermeable fibres formed by mesh-based cylinders. We created four simulation scenes with the same intracellular fraction (fIC=0.74), where each contains specific fibre radius R(=1/2/4/6 µm).

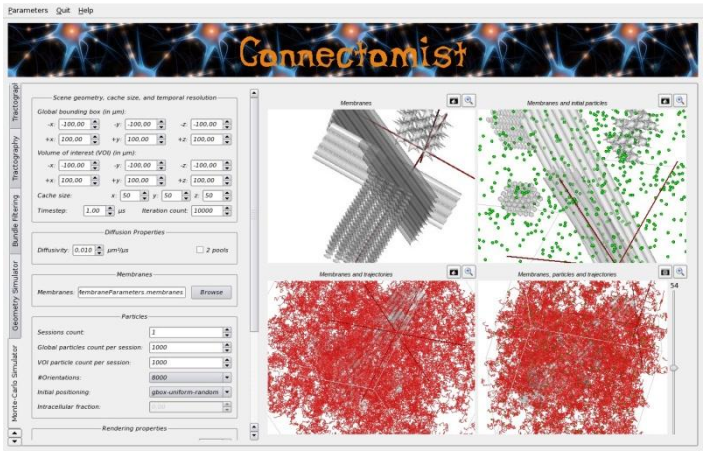


Figure 1: Example of synthetic tissue modelling using the Monte-Carlo simulator developed in the BrainVISA/Connectomist-2.0 software platform

A synthetic MR dataset was obtained by simulating a PGSE sequence with trapezoidal DW gradient pulses. The table below summarizes the list of imaging protocols created to conform to the capability of clinical MR system. Each protocol contains 120 DW acquisitions with different M and N combinations, where M is the number of q-space sampling shells and N is the number of DW gradient orientations per shell. In each protocol, the gradient amplitude and slew rate were fixed at 40 mT/m and 200 T/m/s respectively, while the DW gradient pulse duration (δ) and separation (Δ) were varied simultaneously to keep a constant effective diffusion time (Δeff=Δ–δ/3=50 ms) so as to reach sufficient diffusion sensitizing factors (i.e. b-values) for short δs. Note that all of the b-values used in this study were all clinically achievable. The echo time (TE) determined by the maximum δ and Δ was fixed in each protocol, and a T2 of 70 ms typically found in WM at 3T was used.

Parameter estimation was performed using the Markov Chain Monte Carlo (MCMC) method implemented with Rician noise model to sample the posterior distribution of model parameters developed by DA team.

The table below shows the histograms of R estimates obtained from the posterior distribution for each true radius R, and the table summarizes the mean and standard deviation (σ) of the distributions for each case. All of the protocols accurately estimated large radii (R=4 and 6 µm) but produced a bias for small radii, especially for R=1 µm; nevertheless, it could be still recognized as a small size. For M=3 (i.e. Protocol 1-3), Protocol 3 resulted in better R estimation than other protocols, indicating that moderate to high b-values were important for accurate R mapping. The similar findings were observed when M=4 and 5: Protocol 6&8 utilized higher b-values and resulted in sharper distributions, i.e. lower σ. Protocol 3 (M=3), 6 (M=4), and 8 (M=5) resulted in less overlapping between R=1 and 2 µm, and produced sharper distribution for larger radii. Furthermore, Protocol 3 was better in terms of accuracy and precision, which implied that introducing low b-value shells might spread distribution.

We assessed the feasibility in mapping fibre radii under the constraints of clinical MR systems. Within clinical acceptable acquisition time (~30 minutes), we observed that using three shells with moderate to high b-values (Protocol 3) is potentially sufficient to estimate fibre/cellular sizes with minimum overlapping between distributions. Further work will consider more realistic

biological conditions, such as the effect of size distribution, permeability, and angular dispersion of the fibres.

**Table 1. Clinical PGSE DW MR imaging protocols**

| *Protocol* | M | N | δ (ms) | TE (ms) | *b*-value (s/mm$^2$) |
|---|---|---|---|---|---|
| 1 | 3 | 40 | 4, 8, 12 | 70.5 | 80, 350, 800 |
| 2 | | | 8, 16, 20 | 81.2 | 350, 1430, 2250 |
| 3 | | | 16, 20, 24 | 86.5 | 1430, 2250, 3250 |
| 4 | 4 | 30 | 4, 8, 12, 16 | 75.8 | 80, 350, 800, 1430 |
| 5 | | | 8, 12, 16, 20 | 81.2 | 350, 800, 1430, 2250 |
| 6 | | | 12, 16, 20, 24 | 86.5 | 800, 1430, 2250, 3250 |
| 7 | 5 | 24 | 4, 8, 12,16, 20 | 81.2 | 80, 350, 800, 1430, 2250 |
| 8 | | | 8, 12,16, 20, 24 | 86.5 | 350, 800, 1430, 2250, 3250 |
| 9 | 6 | 20 | 4, 8, 12,16, 20, 24 | 86.5 | 80, 350, 800, 1430, 2250, 3250 |

**Table 2. Mean ± Standard deviations ($\sigma$) of the distributions**

| *Protocol* | *R*=1 µm | *R*=2 µm | *R*=4 µm | *R*=6 µm |
|---|---|---|---|---|
| 1 | 1.54 ± 0.68 | 2.11 ± 0.61 | 4.11 ± 0.68 | 5.70 ± 0.65 |
| 2 | 1.22 ± 0.44 | 1.78 ± 0.33 | 3.91 ± 0.29 | 6.07 ± 0.58 |
| **3** | 1.02 ± 0.31 | 1.86 ± 0.26 | 3.88 ± 0.33 | 5.91 ± 0.34 |
| 4 | 1.07 ± 0.50 | 1.93 ± 0.65 | 3.81 ± 0.50 | 6.11 ± 0.41 |
| 5 | 1.17 ± 0.31 | 1.84 ± 0.53 | 3.93 ± 0.48 | 6.11 ± 0.54 |
| *6* | 1.04 ± 0.27 | 1.78 ± 0.30 | 3.90 ± 0.38 | 6.12 ± 0.44 |
| 7 | 1.29 ± 0.35 | 1.95 ± 0.63 | 3.92 ± 0.44 | 6.22 ± 0.43 |
| *8* | 0.96 ± 0.32 | 1.79 ± 0.26 | 3.92 ± 0.27 | 5.94 ± 0.41 |
| 9 | 1.14 ± 0.37 | 1.69 ± 0.47 | 3.91± 0.35 | 6.00 ± 0.37 |

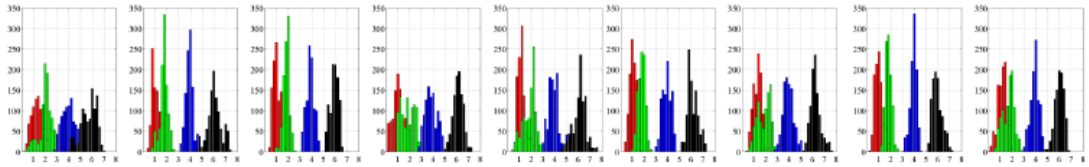

Multiple compartment diffusion modelling

Water diffusion in biological tissues is not free (Gaussian), as the signal attenuation is not mono-exponential with diffusion-weighting (b value). Some groups have successfully characterized this attenuation with a bi-exponential model, which suggests the presence of 2 water pools in slow or intermediate exchange. However, this model is still controversial and the nature of the 2 pools (e.g., membrane-bound and intra/extra-cellular bulk water) remains elusive.

In this part of the WP the group of DB developed a semi-analytical model of multiple compartment diffusion to go beyond Karger's equations and an efficient numerical solution of Bloch-Torrey partial differential equations to provide an efficient hybrid model of the diffusion process enabling fast simulations.

We considered the Bloch-Torrey partial differential equation model (PDE in time and space) for the magnetization and showed that because the diffusion MRI signal is the integral of the magnetization, we can formulate an ordinary differential equation (ODE only in time) directly on the signal. This made the inverse problem of determining biological parameters from the DMRI signal more numerically tractable, as the number of unknowns is vastly reduced. At the same time, the link between the biological properties of diffusion in the different compartments and the overall signal was made more direct and will aide in the more straightforward interpretation of the DMRI signals in terms of the underlying physical properties of water diffusion in tissue. This model is more general than the widely used Karger model because it takes into account the geometry of the cellular structure. Simulations were performed using a random walk Monte Carlo simulator to simulate 3D water molecular diffusion in a bundle of parallel impermeable fibres formed by mesh-based cylinders.

We also proposed a numerical method for solving the Bloch-Torrey partial differential equation in multiple diffusion compartments to compute the bulk magnetization of a sample under the influence of a diffusion gradient. We coupled a mass-conserving finite volume discretization in space with a stable time discretization using an explicit Runge-Kutta-Chebyshev method. We were able to solve the Bloch-Torrey PDE in multiple compartments rapidly and accurately, making it a reasonable candidate as the forward solver in the inner iterative loop of an inverse problem solver going from signals to biological parameters.

Development of a sampling-based probabilistic tractography algorithms

Tractography algorithms use fibre-orientation estimates in each voxel to propagate streamlines through the brain. However, the fibre-orientation estimates are generally calculated using data from a single voxel. Utilising information from neighbouring voxels may improve fibre-orientation estimates. In this work, we develop a new probabilistic tractography framework that:

- uses data sampled from a neighbourhood of voxels to determine the next step in the streamline propagation rather than the data from a single voxel.
- is general to all reconstruction algorithms, including multiple fibre reconstruction techniques such as persistent angular structure (PAS) MRI and QBall.

The algorithm we propose randomly samples a new set of raw diffusion MRI data from the local 8-neighbourhood of voxels at each step of the streamline propagation. The distance between the current end-point of the streamline and the centre of a given voxel in the neighbourhood is used to weight the probability of drawing a sample from that voxel; the closer the end-point is to the centre of a voxel, the higher the probability of drawing a sample from it. The new set of data are then processed using a reconstruction algorithm, such as diffusion tensor imaging (DTI) or PASMRI, to obtain the next fibre-orientation estimate(s). We demonstrate the technique using DTI and the multi-tensor model, although the technique can be used with any reconstruction algorithm.

Poor spatial resolution is a limitation in various diffusion MRI applications, including tractography. A Bayesian latent variables random effects model has been developed for increasing effective spatial resolution, based on a Markov random field treatment in which intrinsic Gaussian autoregressive priors are assigned to the fibre spherical coordinates. The model is used to separate crossing-fibres at the junction between the cingulum and corpus callosum, using diffusion MRI data acquired with a moderate b-value and 20 directions. The analyses were performed using Markov chain Monte Carlo simulation. Results demonstrate that a satisfactory separation of the crossing components can be obtained (King et al ISMRM 2011).

Analysis of the data set collected in WP1

The group of DA has also analyzed the data set collected in WP1 to evaluate the effect of acquisition protocol on the estimates of microstructure features. In collaboration with the Copenhagen (TD) and Tel Aviv groups (YA and YC), the group of DA have acquired fixed monkey brain data and in-vivo rat brain with both rich AxCaliber protocols and economical optimized protocols. The findings demonstrate that we can recover similar trends in white matter microstructure with the more economical acquisition.

Due to the complexity of the diffusion process and its milieu, distinct diffusion compartments can have different frequency signatures, making the HARDI signal spread over multiple frequency bands (Figure 2). Therefore, the group of DB put forth the idea of multiscale analysis with localized basis functions, ensuring that different frequency ranges are probed. With the aim of truthful recovery of fibre orientations, we reconstruct analytically the orientation distribution function (ODF), by incorporating a spherical wavelet transform (SWT) into the Funk–Radon transform. First, we apply and validate our proposed SWT method on real physical phantoms emulating fibre bundle crossings. Then, we apply the SWT method to a real brain data set. For both phantom and real data, we compare the SWT reconstruction with state-of-the-art q-ball imaging and spherical deconvolution reconstruction methods. We demonstrate the algorithm efficiency in diffusion ODF denoising and sharpening that is of particular importance for applications to fibre tracking (especially for probabilistic approaches), and brain connectome mapping. Also, the algorithm results in considerable data compression that could prove

beneficial in applications to fibre bundle segmentation, and for HARDI based white matter morphometry methods.

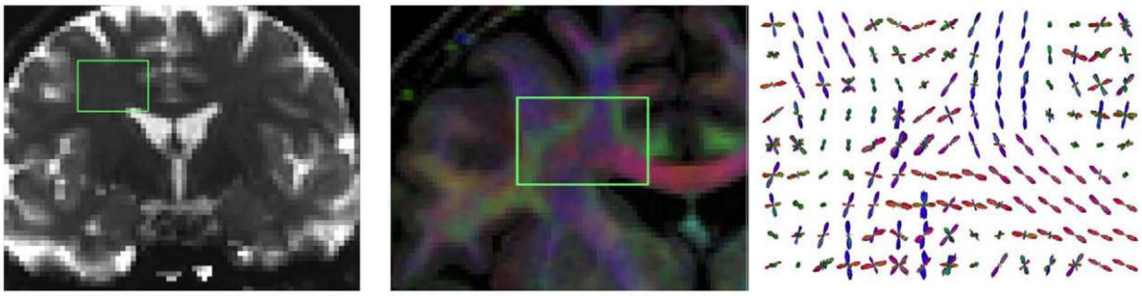

Figure 2. Sparse single-shell HARDI models. T2-weighted image (left), RGB coded tensor map with the region of interest (ROI) (middle), and 3D-rendering of sparse HARDI models from the ROI (right).

**Human AxCaliber Protocol**

One of the main challenges of adapting AxCaliber framework to the human brain is the limitations of clinical scanner. Specifically, the low gradient amplitude is a conceptual limitation as the AxCaliber framework assumes strong diffusion gradient amplitude with relatively short exposure time ($\delta$). To overcome this issue, the group YA have modified the analysis routine to cope with this limitation. The group of YA have replaced Callaghan's formula for diffusion in cylinders with Van-Geldern's one which better fits human scanner experimental set-up. In a preliminary experiment, we have scanned a human subject with an AxCaliber protocol ($\delta$ of 21 ms, four $\Delta$ values= 87.8, 67.8, 47.8, 28.8, maximal gradient strength of 3.65 G/cm applied exactly perpendicular to the corpus callosum) and analyzed it with the conventional AxCaliber framework. Although the experimental protocol still need to be optimized (in terms of signal to noise and other experimental conditions such as b value, TE, TR), we were able to extract the ADD for different parts of the corpus callosum (CC) (Fig. 3) that do resemble the known morphology of fiber composition in the CC.

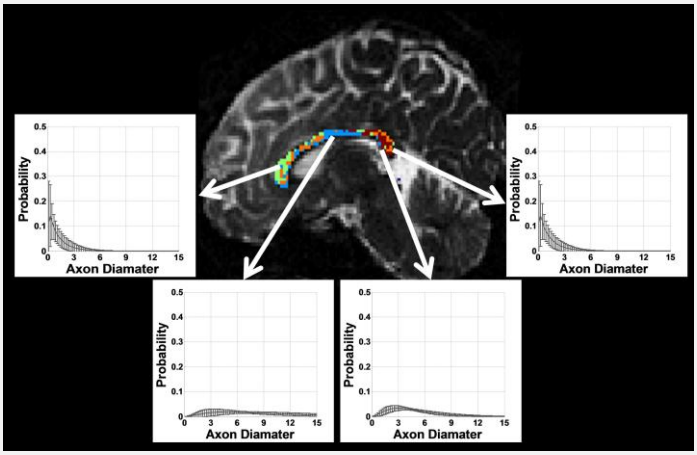


Fig. 3: AxCaliber of the human corpus callosum segmenting it into 4 regions of distinct fiber composition. The genu and splenium show narrow ADD, while the body shows much broader distribution.

## (B) Analysis Routine Optimization

Optimizing micro-structure fitting routines

The group of DA also runs simulation experiments on acquisition protocols other than the ones based on PGSE sequence. In particular, we demonstrate the improved axon diameter estimates using protocols based on optimized general gradient waveforms with simulation, which is subsequently validated on a 9.4T scanner using a capillary phantom.

To overcome some of the issues found by the simulations using current techniques, the group of DA has developed a new white matter tissue model that represents the underlying axonal-orientation distribution with Watson distribution. The Watson model naturally captures the dispersion about the central orientation and is shown, both in simulation and in in vivo human brain data, to provide more sensible axon diameter estimates than the existing techniques.

The group of DA has performed a large scale computational comparison of around 50 different candidate models for the diffusion signal from White matter using high quality specialist measurements at 9.4T. Findings show that three compartments are necessary to explain the signal well. Models that underpin standard techniques like AxCaliber and ActiveAx perform well although improvements are possible.

Optimizing diffusion models

The group of DB, in collaboration with DA's group, examined multi-compartmental systems where the intra-cellular architecture and exchange between the compartments are considered. We build an analytic model that can explain cell characteristic sizes, including the nuclear size, as well as the cell-membrane permeability, the features that are suggested to be related to different tissue pathologies. For example, the nuclear-to-cell ratio is a proven marker of the tumour malignancy grade, while the increase in water permeability has been detected for cells of some pathological tissues. Using this model, an optimized imaging design to measure the relevant microstructure features is delivered. Using Markov Chain Monte-Carlo (MCMC) simulations, we test the feasibility of estimating the proposed model parameters, for technical settings adapted to small animal imaging (17T). We are particularly interested in the cell sub-compartment sizes, cell density, and cell-membrane permeability. The simulation results demonstrate the accuracy of estimating the parameters with both negligible and moderate membrane permeability, and thus suggest the sensitivity to accurately detect the change of particular parameters, e.g., the change of cell-characteristic sizes and membrane permeability. The evidence relating the latter to pathological tissue alterations promotes the potential of the proposed model to provide new microstructural biomarkers (Figure 4).

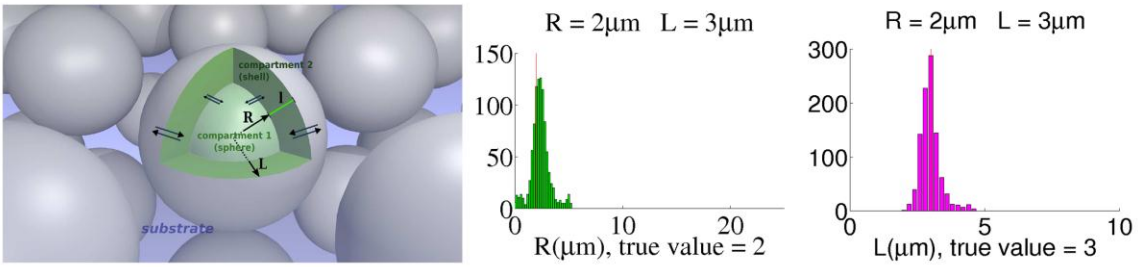


Figure 4. Example of analytic malignant tissue model (left), and corresponding estimates of nuclear radius and cytoplasmic layer thickness (right) from a numerical study of virtual high-field systems (17T), with no exchange between the three water compartments (nuclear, cytoplasmic, and extracellular). [72]

Optical imaging studies suggest that the brain cell swelling is one of the physiological responses associated with neuronal activation. It has been hypothesized that cortical cells swell as a consequence of water infiltration during activation. Le Bihan proposed a simple tissue model to explain the diffusion signal changes accompanying the neuronal activation has been proposed. Three distinct tissue compartments were assumed: the extracellular (EC) compartment; membrane compartment (MC) that accounted for the cell membrane and the water trapped by the electrostatic forces of the membrane (and the associated cytoskeleton); and the intra-cellular (IC) compartment that accounted for the remaining cytoplasmic water. Cell swelling during activation is reflected in the MC compartment enlargement. A biphasic diffusion model was employed to explain the overall diffusion signal coming from all three tissue compartments: the first phase was related to the signal coming from the merged "free" water pool, i.e. the sum of the signals from the EC and IC compartments; the second phase was related to the signal coming from the "membrane-bound" water pool (MC). The MC enlargement during activation induces changes of the diffusion signal. We propose a geometric model for the presumed tissue model, and an analytic diffusion signal model to explain the signal coming from the assumed geometry. An optimized imaging protocol for this model is delivered. The accuracy to estimate the MC size before and during the activation, and thus the sensitivity of diffusion signal to changes in MC size during activation is tested using the optimized protocol. The simulation results suggest the feasibility to detect and evaluate MC size changes on 7Tesla human in vivo systems.

Diffusion imaging Acquisition Optimization

Echo-planar imaging (EPI) is a widely used technique in functional MRI (fMRI). The EPI extension Real-time diffusion-weighted (DW) Magnetic Resonance Imaging (rt-dMRI), introduced by Poupon in 2008, performs diffusion tensor (DTI) and High Angular Resolution Diffusion (HARDI) imaging on the fly, during the acquisition (Figure 8). This technique is fully dedicated to clinical applications, where scan duration is a limiting factor, and produces in real-time the maps of all the indices and distribution functions relating to HARDI or Hybrid Diffusion (HYDI) models (such as the General Fractional Anisotropy (GFA), the Orientation Distribution Function (ODF) and the Fibre Orientation Distribution (FOD)). Further progress was made to optimize the orientation set and to detect the motion on-line. Nonetheless, the well-known dMRI problem of low SNR at high b-values retains unsolved.

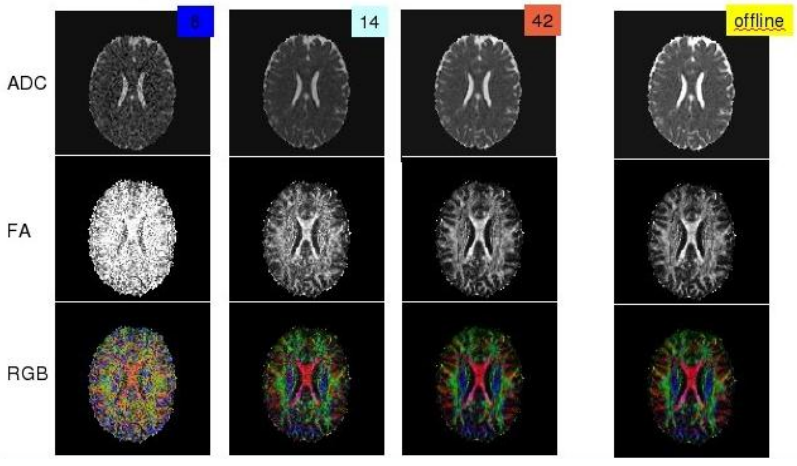


Figure 5: Example of real-time DTI scan depicting the incremental estimates of the ADC, FA and RGB maps obtained after 6, 14, 42 diffusion directions respectively, and compared with the standard offline reconstruction

We have proposed a novel algorithm to remove Rician noise from diffusion-weighted data in real-time (Figure 6). This novel technique was embedded with the real-time dMRI platform developed by the DB team in 2008. The method was employed to create a dedicated application that corrects Rician noise and estimates fibre orientation distribution functions inside volumes of human brain images, as well as the standard diffusion maps used for clinical diagnosis. The tool was successfully validated on ultra-low SNR DW data obtained during an in vivo experiment that was performed on a healthy volunteer. This tool now allows for multiple-shell HYDI imaging at very high b-values that enables a plethora of new applications focused on the inference of the ensemble average propagator, providing much richer information than orientation distribution functions.

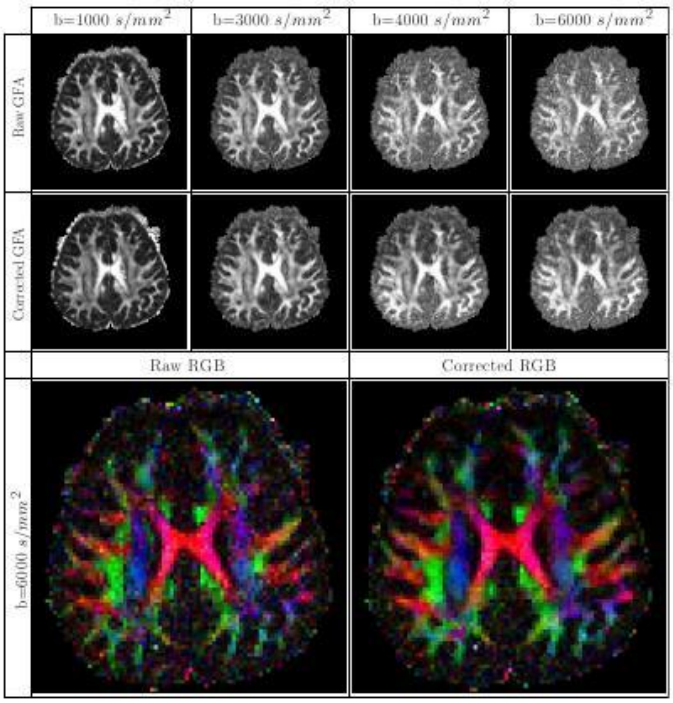


Figure 6: Raw and noise-corrected GFA and RGB maps obtained for 4 different b-values b=1000/3000/ 4000/6000s/mm² performed on a 3T MRI system, on a healthy volunteer, demonstrating the enhancement of the real-time Rician noise correction when the b-value is increased.

## Relevant Publications:

The outcomes of this part of the project are delivered in the following publications (attached at the following pages):

1. Panagiotaki E, Schneider T, Siow B, Hall MG, Lythgoe MF, Alexander DC. Compartment models of the diffusion MR signal in brain white matter: A taxonomy and comparison. Neuroimage. 2011 Oct 7.
2. Panagiotaki E, Hall MG, Zhang H, Siow B, Lythgoe MF, Alexander DC. High-fidelity meshes from tissue samples for diffusion MRI simulations. Med Image Comput Comput Assist Interv. 2010;13(Pt 2):404-11.
3. Zhang H, Dyrby TB, Alexander DC. Axon diameter mapping in crossing fibers with diffusion MRI. Med Image Comput Comput Assist Interv. 2011;14(Pt 2):82-9.
4. Feng-Lei Zhou, Penny L. Hubbard, Stephen J. Eichhorn, Geoffrey J.M. Parker. Jet deposition in near-field electrospinning of patterned polycaprolactone and sugar-polycaprolactone coreeshell

fibres. Polymer 52 (2011) 3603-3610

5. King, MD., Alexander, DC., Gadian, DG., Clark, CA. A Bayesian Random Effects Model for Enhancing Resolution in Diffusion MRI in ISMRM 19th Annual Meeting Proceedings, 2011, Montréal, page 1925.
6. Yeh C.-H, Tournier J.-D, Cho K-H, Poupon C, Lin C.-P, 2009. Evaluation of angular uncertainties of Q-space diffusion MRI under finite gradient pulse widths: a phantom study. In proceedings 17th ISMRM 2009, Haiwai, Honolulu. 2009, abstract number 3550
7. Yeh CH, Le Bihan D, Li JR, Mangin JF, Lin CP, Poupon C. Monte-Carlo simulation software dedicated to diffusion weighted MR experiments in neural media. In proceedings 16th HBM, 2010 (Barcelone, Spain)
8. Yeh CH, Le Bihan D, Li JR, Mangin JF, Lin CP, Poupon C. Monte-Carlo simulation software dedicated to diffusion weighted MR experiments in neural media. In Proceedings ISMRM 2010 (Stockholm, Sweden), abstract number 5762.
9. Poupon C, Laribière L, Tournier G, Bernard J, Fournier D, Fillard P, Descoteaux M, Mangin JF. A diffusion hardware phantom looking like a coronal brain slice. In Proceedings ISMRM 2010 (Stockholm, Sweden), abstract number 1270.
10. Yeh CH, Kezele I, Alexander D, Schmitt B, Li JR, Le Bihan D, Lin CP, Poupon C. Evaluation of fiber radius mapping using diffusion MRI under clinical system constraints". In Proceedings 19th ISMRM, Montreal, Canada, 2011, abstract number 2017
11. Aso T, Poupon C, Urayama S,Kukuyama H, Le Bihan D, 2009. Evaluation of diffusion FMRI (DfMRI) with short event related paradigms. In proceedings 17th ISMRM 2009, Haiwai, Honolulu. Abstract number 1573
12. Le Bihan D, Aso T, Urayama S, Poupon C, Sawamoto N, Aso K, Fukuyama H. How vascular effects contribute to heavily diffusion-weighted FMRI signal. In proceedings 17th ISMRM 2009, Haiwai, Honolulu. 2009, abstract number 1569
13. Li JR, Poupon C, Le Bihan D. A theoretical framework to model diffusion MRI signals taking into account cell membranes. In Proceedings ISMRM 2010 (Stockholm, Sweden), abstract number 5762.
14. Li JR, Calhoun D, Yeh CH, Poupon C, Le Bihan D. Efficient Numerical Solution of the Bloch-Torrey Equation for Modeling multiple compartment diffusion". In Proceedings 19th ISMRM Conference, Montreal, 2011, abstract number 3946.
15. D. Le Bihan, O. Joly, T. Aso, L Uhryg, C Poupon, N. Tani, H Iwamaro, S.-H urayama, B Jarraya. Brain Tissue Water Comes in 2 Pools: Evidence from Diffusion & R2 Measurements with USPIOs in Non Human Primates. In Proceedings 19th ISMRM Conference, Montreal, 2011, abstract number 3952.
16. Kezele I, Descoteaux M, Poupon C, Poupon F, Mangin J-F. Spherical wavelet transform for ODF sharpening. Medical Image Analysis. 2010, 14(3):332-342
17. Kezele I, Poupon C, Descoteaux M, Poupon F, Mangin J.-F. Importance of multiscale analysis in HARDI studies. In proceedings 17th ISMRM 2009, Haiwai, Honolulu. 2009, abstract number 1384
18. Descoteaux M, Deriche R, Le Bihan D, Mangin J-F, Poupon C. Multiple q-shell diffusion propagator imaging. Medical Image Analysis. 2011, Aug ; 15(4):603-21
19. Descoteaux M, Deriche R, Le Bihan D, Mangin J.-F, Poupon C. Diffusion Propagator Imaging: using the Laplace equation anf multiple shell acquisitions to reconstruct the diffusion propagator. Inf

Process Medical Imaging. 2009, 21:1-13 Best Paper Award

20. Descoteaux M, Mangin J.-F, Poupon C. Diffusion Propagator Imaging: a novel technique for reconstructing the diffusion propagator from multiple shell acquisitions.. In proceedings 17th ISMRM 2009, Haiwai, Honolulu. 2009, abstract number 364
21. Descoteaux M, Cho K.-H, Chao Y.-P, Yeh C.-H, Mangin J.-F, Lin C.-P, Poupon C. Diffusion Propagator Imaging: an alternative to Diffusion Spectrum Imaging. In proceedings 17th ISMRM 2009, Haiwai, Honolulu. 2009, abstract number 1391
22. Kezele I, Alexander DC, Batchelor P, Mangin JF, Le Bihan D, Poupon C. Measuring microstructural features related to neuronal activation using diffusion MRI and three-compartmental diffusion models: a feasibility study. In Proceedings ISMRM 2010 (Stockholm, Sweden)
23. Kezele I, Batchelor P, Poupon C, Mangin JF, Le Bihan D, Alexander DC. Feasibility of measuring microstructural features of systems with intermediate exchange and sub-cellular compartmentalization using diffusion MRI. In Proceedings ISMRM 2010 (Stockholm, Sweden)
24. Brion V, Kezele I, Descoteaux M, Mangin J.-F, Poupon C, 2009. Rician denoising dedicated to single-shell diffusion-weighted MR data using spherical harmonics: impact on fibre orientation distribution maps. In Proceedings ESMRMB 2009, Antalya.
25. Brion V, Kezele I, Riff O, Descoteaux M, Mangin JF, Poupon C, Poupon F. Real-time Rician noise correction applied to real-time HARDI and HYDI. Med. Image. Computing Assist Interv. 2010, Workshop Computational Diffusion MRI
26. Brion V, Kezele I, Riff O, Descoteaux M, Mangin JF, Poupon C, Poupon F. Real-time Rician noise correction applied to real-time HARDI and HYDI. Med. Image. Computing Assist Interv. 2010, Workshop Computational Diffusion MRI
27. Poupon C, Dubois J, Marrakchi-Kacem L, Brion V, Mangin JF, Poupon F. Real-time EPI T1, T2 and T2* mapping at 3T. In Proceedings ISMRM 2010 (Stockholm, Sweden)
28. Brion V, Riff O, Kezele I, Descoteaux M, Le Bihan D, Mangin JF, Poupon C, Poupon F. Real-Time Rician Noise Correction Applied to Real-Time HARDI and HYDI". In Proceedings 19th ISMRM 2011 Conference, Montreal, abstract number 1930.
29. Parallet MRI noise correction: an extension of the LMMSE to non cenral chi dsitributions. Brion V, Poupon C, Riff O, Aja-Fernández S, Tristán-Vega A, Mangin JF, Le Bihan D, Poupon F. Med Image Comput Comput Assist Interv. 2011;14(Pt 2):226-33.